

PAPER

Constraint dependence of pressure on a passive probe in an active bath

To cite this article: Peng Liu *et al* 2023 *J. Phys.: Condens. Matter* **35** 445102

View the [article online](#) for updates and enhancements.

You may also like

- [Towards the development of active compression bandages using dielectric elastomer actuators](#)
S Pourazadi, S Ahmadi and C Menon
- [Fabrication and performance analysis of a DEA cuff designed for dry-suit applications](#)
S Ahmadi, A Camacho Mattos, A Barbazza et al.
- [Space charge dynamics of epoxy/micro- \$\text{Al}_2\text{O}_3\$ composites under multi-physical fields](#)
Zongliang Xie, Xi Pang, Tianlei Xu et al.

Constraint dependence of pressure on a passive probe in an active bath

Peng Liu^{1,2,6} , Longfei Li^{1,6}, Luhui Ning^{1,3}, Ning Zheng^{2,*} and Mingcheng Yang^{1,4,5,*}

¹ Beijing National Laboratory for Condensed Matter Physics and Laboratory of Soft Matter Physics, Institute of Physics, Chinese Academy of Sciences, Beijing 100190, People's Republic of China

² School of Physics, Beijing Institute of Technology, Beijing 100081, People's Republic of China

³ Wenzhou Institute, University of Chinese Academy of Sciences, Wenzhou, Zhejiang 325001, People's Republic of China

⁴ School of Physical Sciences, University of Chinese Academy of Sciences, Beijing 100049, People's Republic of China

⁵ Songshan Lake Materials Laboratory, Dongguan, Guangdong 523808, People's Republic of China

⁶ These authors contributed equally to this work.

E-mail: ningzheng@bit.edu.cn and mcyang@iphy.ac.cn

Received 12 April 2023, revised 6 July 2023

Accepted for publication 28 July 2023

Published 7 August 2023



Abstract

Mechanical pressure in active matter is generally not a state variable and possesses abnormal properties, in stark contrast to equilibrium systems. We here show that the pressure on a passive probe exerted by an active fluid even depends on external constraints on the probe by means of simulation and theory, implying that the mechanical pressure is not an intrinsic physical quantity of active systems. The active mechanical pressure on the passive probe significantly increases and saturates as its elastic constraint (realized by a trap potential) or kinematic constraint (realized by environmental friction) strengthens. The microscopic origin for the constraint-dependent pressure is that the constraints influence the probe dynamics, and hence change the frequency and intensity of the collisions between the probe and active particles. Our findings not only greatly advance the understanding of active mechanical pressure but also provide a new way to *in situ* tune it.

Supplementary material for this article is available [online](#)

Keywords: soft matter, active matter, constraint, active pressure

(Some figures may appear in colour only in the online journal)

1. Introduction

Active matter, such as bacteria colonies [1–3] and synthetic active colloids [4–10], often exhibits exotic nonequilibrium phenomena [11–20] due to its constituents persistently converting stored or ambient energy into self-propulsion. To better understand and explore the unusual features of active matter, many fundamental physical concepts in thermal bath have been generalized to active bath [21–29]. Especially,

mechanical pressure in active systems has attracted considerable attention and been extensively investigated [3, 16, 25, 26, 30–63]. The active mechanical pressure has been shown to not only play an important role in inducing collective motion of active agents [31, 32] and unidirectional transport of immersed asymmetric passive objects [3, 33–37], but also provide a useful starting point to study the rheological properties [38, 39], interfacial tension [40–42] and phase behaviors of active matter [16, 25, 26, 43–63].

Unlike the pressure in thermal bath, the mechanical pressure is not a state variable for generic active fluids and

* Authors to whom any correspondence should be addressed.

strikingly depends on the wall interaction details [64–74]. An exception is the mechanical pressure on a flat wall exerted by the active Brownian spheres free of any torque coupling (ABPs) [25, 43, 44, 48, 75, 76]; while, for curved boundary walls, the mechanical pressure hinges on the boundary curvature [72, 77–79]. Given the lack of an equation of state in general, a possible second-best situation could be that a generic probe, with certain geometry and interaction detail, experiences a unique mechanical pressure in a certain active fluid. Such a situation admits an unambiguous determination of active pressure on the probe, independent of the measurement strategy. This seemingly natural situation is not necessarily always valid, as recent studies have revealed that the active depletion force/torque and active noise experienced by passive probes in active baths sensitively depend on their measurement schemes [80–83], reflected in their dependences on external constraints. Thus, an important question is how the active pressure on a passive probe is affected by its external constraint, which is often correlated with the measurement strategy.

In this work, we quantify the mechanical pressure on a passive colloidal sphere trapped by an external harmonic potential in a fluid of ABPs, using computer simulation and theory. The results show that the pressure experienced by the passive probe is sensitive to the degree of the constraint, and increases and then saturates with the trap stiffness. In other words, the value of mechanical pressure is dependent on how tightly the probe particle is caught when measuring. This counterintuitive result originates from the effect of the constraint on the probe dynamics, which changes the frequency and intensity of the collisions between the probe and active particles. This scenario is further confirmed by varying the probe dynamics through the environmental friction coefficient. Our findings thus mean that the active mechanical pressure is generally not an intrinsically physical quantity.

2. Simulation method

We consider a two-dimensional (2D) active bath consisting of 2000 ABPs with a diameter of σ^a and one large passive probe with a diameter of $\sigma^p = 3\sigma^a$. They interact repulsively through a truncated and shifted Lennard–Jones-type potential $U(r) = 4\epsilon[(\sigma/r)^{24} - (\sigma/r)^{12}] + \epsilon$, with the center-to-center particle distance r and a cutoff at $r = 2^{1/12}\sigma$, beyond which $U(r) = 0$. Here, the σ is defined as the interaction diameter and ϵ determines the interaction strength, equal to the thermal energy $k_B T$. We use the overdamped Langevin equation to evolve the translational and rotational motion of the active particle i ,

$$\begin{aligned} \dot{\mathbf{r}}_i^a &= v_0 \mathbf{u}(\theta_i) + \mu \mathbf{F}^p(\mathbf{r}^p - \mathbf{r}_i^a) + \mu \sum_j \mathbf{F}_{ij}^a + \sqrt{2D_t} \boldsymbol{\eta}_i, \\ \dot{\theta}_i &= \sqrt{2D_r} \xi_i. \end{aligned} \quad (1)$$

Here, \mathbf{r}_i^a represents the position of the i th active particle, v_0 , the ratio of the driving force F_d to translational friction coefficient γ^a , is the self-propelled velocity with direction $\mathbf{u}(\theta_i) =$

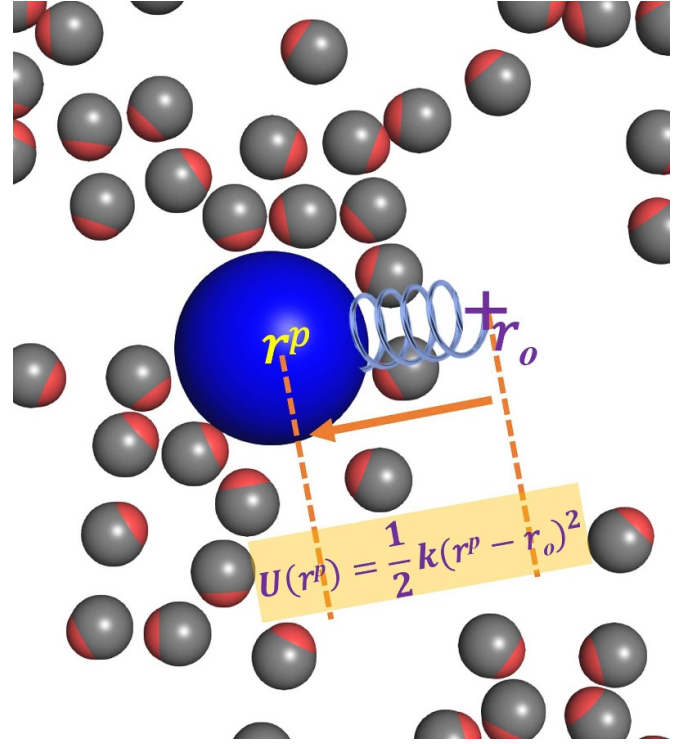


Figure 1. Sketch of the simulation system, consisting of small active particles self-propelling towards the red side, and a passive spherical probe (blue) constrained by an external harmonic potential $U(\mathbf{r}^p) = \frac{1}{2}k(\mathbf{r}^p - \mathbf{r}_o)^2$.

$[\cos \theta_i, \sin \theta_i]^T$. $\mathbf{F}^p(\mathbf{r}^p - \mathbf{r}_i^a)$ and \mathbf{F}_{ij}^a represent the steric interaction forces exerted on the active particle i by the passive probe and the j th active particle, respectively. $\boldsymbol{\eta}_i$ and ξ_i represent independent Gaussian-distributed white noises with zero mean and correlation $\delta(t)$. In addition, $D_t = \mu k_B T$ ($D_r = \mu_r k_B T$) corresponds to the translational (rotational) diffusion coefficient, where $\mu = 1/\gamma^a$ ($\mu_r = 1/\gamma_r, \gamma_r = \frac{1}{3}\sigma^{a2}\gamma^a$, with γ_r the rotational friction coefficient) is the mobility of the active particles. Unless otherwise stated, in simulations, the dimensionless driving force of the active particle is set to $F_d \sigma^a / k_B T = 20$, close to the one of the bacterium, and the packing fraction of ABPs is taken as $\rho_p = 0.3$ to avoid the formation of large clusters.

The evolution of the large passive probe is also described by the overdamped Langevin equation,

$$\dot{\mathbf{r}}^p = -\mu^p \sum_j \mathbf{F}^p(\mathbf{r}^p - \mathbf{r}_j^a) + \sqrt{2D_t^p} \boldsymbol{\eta}^p - k(\mathbf{r}^p - \mathbf{r}_o). \quad (2)$$

Similarly, \mathbf{r}^p and $D_t^p = \mu^p k_B T$ ($\mu^p = 1/\gamma^p$, with γ^p the translational friction coefficient of the probe) refer to the position and translational diffusion coefficient of the passive probe, respectively, and $\boldsymbol{\eta}^p$ to the Gaussian-distributed white noise. Besides the interactions with the ABPs, the probe is constrained by an external harmonic potential $U(\mathbf{r}^p) = \frac{1}{2}k(\mathbf{r}^p - \mathbf{r}_o)^2$, where \mathbf{r}_o is the trap center, as sketched in figure 1. In this work, the integration time step to solve the equations of motion is $\Delta t = 10^{-3} \times \sigma^a \sqrt{m/\epsilon}$. Each data point in the figure is obtained through 16 trajectories, and each trajectory consists

of 3×10^8 steps. A frame is extracted every 10 steps for data analysis. Throughout the manuscript, we employ the standard reduced simulation units, in which m , σ^a and ϵ are respectively taken as the unit of mass, length and energy.

3. Results and discussions

3.1. Elastic constraint

In the 2D active fluid, the mechanical pressure on the spherical passive probe reads, $P = \int_0^\infty F^p(r)\rho(r)dr$, with $\rho(r)$ the local number density of ABPs [79]. Figure 2(a) shows that the pressure P experienced by the passive particle monotonically increases as the trap stiffness k rises. For larger k , the pressure saturates, with a value corresponding to that of the completely fixed probe (the red dashed line). The external trap-dependence of P is fundamentally different from the case of equilibrium systems, in which the pressure does not hinge on the probe dynamics. In the present active fluid, increasing constraint make the trapped probe difficult to move (escape) when encountering the persistent collisions from surrounding ABPs, thus enhancing the frequency of the collisions between the probe and ABPs (namely, the mean number of ABPs simultaneously interacting with the probe), as verified by the results in figure 2(b). The dependence on the local number density of ABPs is similar to the recent study by Paul *et al*, where the particle density around the probe is shown to have a direct link with the net force experienced by the probe in an active bath [84]. To rule out the possibility that the constraint-dependent pressure arises from the correlation between the ABPs, we also implement simulations for non-interacting (ideal) ABPs. The results, plotted in figures 2(c) and (d), are qualitatively consistent with those for interacting ABPs (figures 2(a) and (b)).

Besides the collision frequency (figure 2(b)), the intensity of the collisions between the probe and ABPs also increases with k , which can be quantified by the average active pressure exerted on the passive particle by a single ABP, P_s . Figure 2(e) displays that P_s monotonically increases with the trap stiffness until reaches saturation, which provides an additional contribution to the constraint dependence of the pressure. A minimal theory is developed to elucidate the effect of constraint on the collision intensity, where the interacting process between the ABPs and probe is approximated as a head-on collision, with the ABP orientation parallel to the vector connecting the ABP and probe. Before the collision, the large probe rests at the trap center; while, after the collision, it moves together with the active particle during a rotational relaxation timescale, $\tau_r = \gamma_r/k_B T$. Ignoring mutiparticle collisions, the overdamped equation of motion of the probe during the collision process reads,

$$(\gamma^p + \gamma^a)\dot{\mathbf{r}}^p = -k\mathbf{r}^p + \mathbf{F}_d. \quad (3)$$

Here, $\mathbf{F}_d - \gamma^a\dot{\mathbf{r}}^p$ corresponds to the impact force exerted on the large probe by the active particle, with the stochastic force

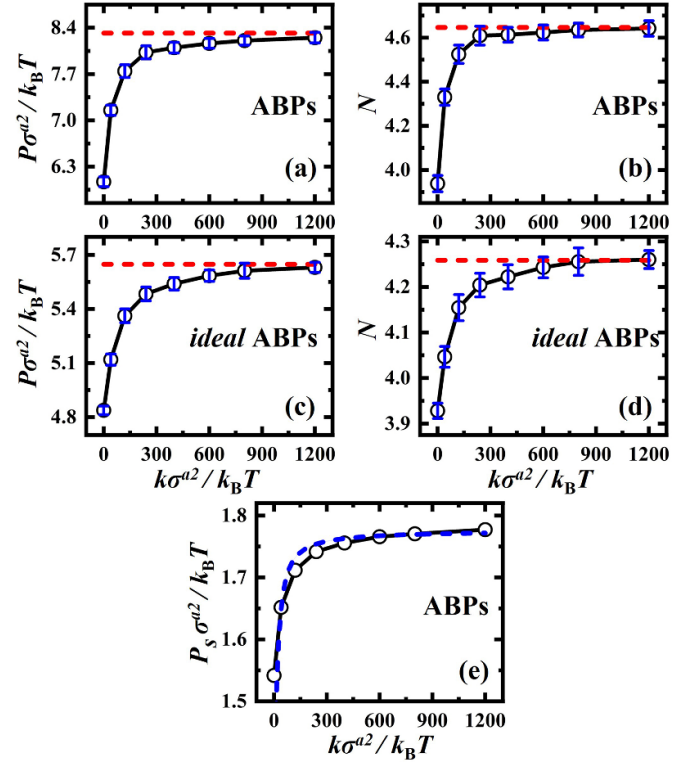


Figure 2. (a) Reduced mechanical pressure P on the passive probe and (b) the mean number N of ABPs simultaneously interacting with the probe as functions of the trap stiffness k . (c) and (d) show the corresponding results for ideal ABPs. The result for the fixed passive probe is indicated by the red dashed lines, and the simulation results are presented with error bars. (e) The average pressure exerted on the probe by a single ABP, with the blue dashed line representing the fitting from equation (5).

omitted. Solving equation (3), the trajectory of the large passive particle is,

$$\mathbf{r}^p(t) = \frac{\mathbf{F}_d}{k} \left[1 - e^{-kt/(\gamma^p + \gamma^a)} \right]. \quad (4)$$

The active pressure on the probe originates from the persistent collision from the ABP and is proportional to the impact force $P_s \sim \mathbf{F}_d - \gamma^a\dot{\mathbf{r}}^p$. After averaging P_s over a timescale τ_r , we have

$$\begin{aligned} P_s &\sim \frac{1}{\pi\sigma^p} \frac{1}{\tau_r} \int_0^{\tau_r} (\mathbf{F}_d - \gamma^a\dot{\mathbf{r}}^p) dt \\ &= C_1 \frac{1}{\pi\sigma^p} \frac{F_d}{\tau_r} \left(\tau_r + \frac{\gamma^a}{k} e^{-k\tau_r/(\gamma^p + \gamma^a)} - \frac{\gamma^a}{k} \right), \end{aligned} \quad (5)$$

with an unknown prefactor C_1 . This approximate theoretical calculation, based on equation (5) with the fitting parameter $C_1 = 0.84$, is well consistent with the direct simulation measurement, as shown in figure 2(e). In addition, the pressure experienced by the probe reduces with the increasing noise, originating from the decreasing persistence length and hence the weakening accumulation of ABPs. The corresponding results have been provided in the supplementary material.

We have so far demonstrated the mechanical pressure exerted on a certain probe in the active fluid is not unique, and

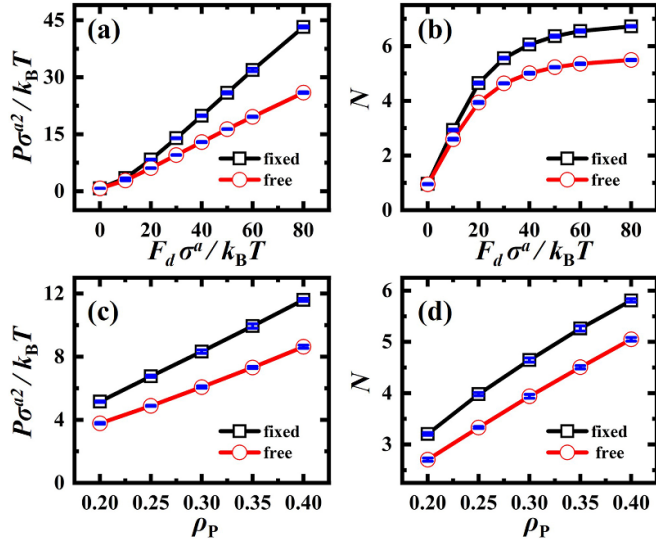


Figure 3. Reduced mechanical pressure P experienced by the fixed and free passive probes (a) and the corresponding mean number N of ABPs simultaneously interacting with the probe (b) as functions of F_d . For (c) and (d), P and N both vary with the packing fractions. In (a) and (b), $\rho_p = 0.3$, while in (c) and (d), $F_d \sigma^a / k_B T = 20$. The simulation results are presented with error bars.

its magnitude is dependent on how tightly the probe particle is caught. In the following, we focus on two extreme cases: a freely moving probe and a fixed probe, and explore their active pressures for various F_d and ρ_p . Figure 3(a) shows that the pressure experienced by the fixed probe is the same as the free one when $F_d = 0$, corresponding to an equilibrium thermal bath. In this case, the pressure is an intrinsic thermodynamic quantity, which does not depend on the probe dynamics hence the external constraint on the probe. Nevertheless, the pressure gap between the fixed and free cases gradually enlarges with the activity of ABPs, highlighting the nonzero pressure gap is completely an active effect. The systems are limited in the regime of relatively low activities and densities, not high enough to induce the motility-induced phase separation (MIPS) [85]. Given the absence of MIPS, when the activity of the active particles is increased, there are two physical effects at play. First, the collision intensity between the active particles and the probe is enhanced, resulting in a significant increase in measured pressure, as illustrated in figure 3(a). Second, the increased activity produces a longer persistent length of the ABP, such that more ABPs accumulate on the probe surface, leading to an enhanced collision frequency between the probe and ABPs, as shown in figure 3(b). As a result, the measured pressure significantly increases with the activity. Furthermore, we measure the P and N for the fixed and free probes as a function of ρ_p with $F_d \sigma^a / k_B T = 20$, as plotted in figures 3(c) and (d). Both the P and N gaps increase with the packing fraction of ABPs, as the persistent ABP-probe collisions become more frequently.

3.2. Kinetic constraint

The constraint dependence of the pressure essentially results from the fact that the active pressure on the probe depends

on the probe dynamics. Besides the external trap, the environmental friction serves as a kinetic constraint that effectively influences the probe dynamics. Thus, it can be expected that the active pressure on a free probe will change with its friction coefficient from the environment, γ^p . Figures 4(a), (b) and (e) separately plot the P , N and P_s as a function of the frictional coefficient γ^p , exhibiting a trend similar to the k -dependence in figures 2(a), (b) and (e). In particular, the mechanical pressure on the free probe with a very large γ^p converges to the value of the fixed probe, since large γ^p and k both substantially prevent the passive probe from escaping from the persistent active collisions. In this sense, the elastic trap and the kinetic constraint play the same role in the determination of active pressure. Consequently, for a sufficiently big probe that has a very large γ^p , its mechanical pressure does not depend on the external constraint any more, such that a unique mechanical pressure can be measured. For comparison, the results for the ideal ABPs are provided in figures 4(c) and (d), which qualitatively agree with those for interacting ABPs shown in figures 4(a) and (b).

Following the above theoretical approximation for the elastic trap (equations (3)–(5)), we can similarly estimate the active pressure exerted on the free probe by a single ABP for different kinetic constraints. The resulting pressure expression is

$$P_s = C_2 \frac{F_d}{\pi \sigma^p} \left(1 - \frac{\gamma^a}{\gamma^p + \gamma^a} \right), \quad (6)$$

with a fitting parameter C_2 . Equation (6) indicates that the P_s increases until saturation with γ^p and it well describes the simulation results with the parameter $C_2 = 0.85$ (blue dashed line in figure 4(e)). Remarkably, for the best fittings, the prefactor C_1 in equation (5) (elastic trap) is almost identical to C_2 in equation (6) (kinetic constraint), suggesting they share a similar physical origin. Moreover, the good agreement between the simulation results and equations (5) and (6) means that the minimal theoretical treatment above captures the essence of the constraint dependence of the active mechanical pressure.

For the case of kinetic constraint, the system is translationally invariant, which thus allows us to derive an exact expression for the mechanical pressure on the free probe. Based on the overdamped Langevin equations of the ideal active system, namely $\mathbf{F}_{ij}^a \equiv 0$ in equation (1), one can obtain the corresponding Smoluchowski equation [43, 86]

$$\begin{aligned} & \frac{d\hat{\psi}(\mathbf{r}^a, \theta, \mathbf{r}^p, t)}{dt} \\ &= -\nabla_{\mathbf{r}^a} \cdot [v_0 \mathbf{u}(\theta) + \mu \mathbf{F}^p(\mathbf{r}^p - \mathbf{r}^a)] \hat{\psi} \\ & \quad - \nabla_{\mathbf{r}^p} \cdot \left[-\mu^p \int \mathbf{F}^p(\mathbf{r}^p - \mathbf{r}^{a'}) \int \hat{\psi}(\mathbf{r}^{a'}, \theta', \mathbf{r}^p, t) d\theta' d^2 \mathbf{r}^{a'} \right] \hat{\psi} \\ & \quad + D_t \nabla_{\mathbf{r}^a}^2 \hat{\psi} + D_r \frac{d^2 \hat{\psi}}{d\theta^2} + D_t^p \nabla_{\mathbf{r}^p}^2 \hat{\psi}, \end{aligned} \quad (7)$$

where $\hat{\psi}(\mathbf{r}^a, \theta, \mathbf{r}^p, t)$ denotes the fluctuating probability distribution of finding the passive probe at \mathbf{r}^p and active particles at \mathbf{r}^a with the orientation θ at time t .

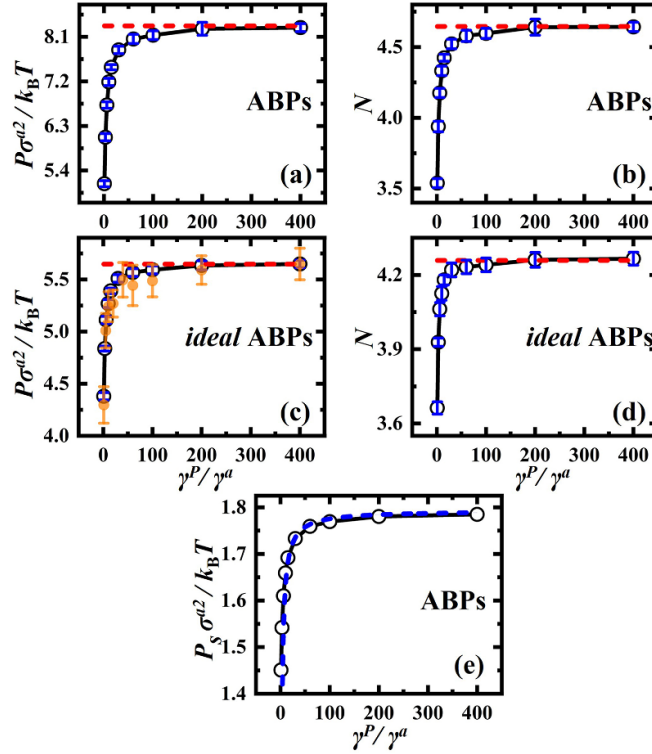


Figure 4. Reduced pressure P experienced by the free passive probe (a) and the mean number N of ABPs simultaneously interacting with the probe (b) as a function of γ^p . (c) and (d) are the cases of ideal ABPs corresponding to (a) and (b), respectively, and the orange circles in (c) are obtained from equation (8). The red dashed lines refer to the pressure on the fixed probe, and the simulation results are presented with error bars. (e) Active pressure on the free probe exerted by a single active particle, where the circle and blue dashed line are obtained from the simulation and the fitting based on equation (6), respectively. Here, $\rho_p = 0.3$ and $F_d\sigma^a/k_B T = 20$ are used.

For convenience, we define $\varphi = \theta - \alpha$ and $\mathbf{n}(\mathbf{r}) = [\cos\alpha, \sin\alpha]^T$, where α is the angle between $\mathbf{r}_i^a - \mathbf{r}^p$ and a fixed arbitrary axis. According to equation (7) and the derivation method used in previous [79, 87], we can obtain the expression for the pressure on the passive probe in an ideal active bath,

$$\begin{aligned}
 P = & \left[\frac{v_0^2}{2\mu D_r} + \frac{D_r + D_t^p}{\mu} \right] \rho(\infty) + \frac{v_0^2}{\mu D_r} \int_0^\infty q \frac{dr}{r} \\
 & + \frac{v_0}{D_r} \int_0^\infty m F^p(r) \frac{dr}{r} + \frac{\mu^p v_0}{\mu D_r} \int_0^\infty \left\langle \mathbf{A} \cdot \mathbf{n}(\mathbf{r}) \int_0^{2\pi} \hat{\psi} \cos \varphi d\theta \right\rangle \\
 & - \frac{\mu^p}{\mu} \int_0^\infty \left\langle \mathbf{A} \cdot \mathbf{n}(\mathbf{r}) \int_0^{2\pi} \hat{\psi} d\theta \right\rangle dr. \quad (8)
 \end{aligned}$$

Here, $\rho(\infty)$ is the number density of active particles far away from the passive probe, $m = \langle \int_0^{2\pi} \cos \varphi \hat{\psi} d\varphi \rangle$ and $q = \langle \int_0^{2\pi} \cos 2\varphi \hat{\psi} d\varphi \rangle$ separately signify the ensemble averages of the first and second moments of the probability density function $\hat{\psi}$, and $\mathbf{A} = \int \mathbf{F}^p(\mathbf{r}') \int \hat{\psi}(\mathbf{r}', \theta', t) d\theta' d^2\mathbf{r}'$ is opposite to the force exerted on the probe by all ideal ABPs. More derivation details are provided in the supplementary material. Equation (8) shows that the mechanical pressure on the probe generally relies on γ_p , unless the terms containing μ_p coincidentally cancel each other, as in the case of thermal bath.

Each term of equation (8) can be determined from independent simulations, and the thus-obtained pressure is in quantitative agreement with the direct simulation measurement, as displayed in figure 4(c).

4. Conclusion

We perform simulations and theoretical calculations to examine the influence of constraints on the active mechanical pressure experienced by a passive probe immersed in a fluid of ABPs, considering both external elastic trap and kinetic constraint induced by environmental friction. We find that the active pressure highly depends on the degree of external constraint (and hence the probe dynamics) for weak constraints, where the probe undergoes significant motion due to the persistent collisions from active particles, and saturates at sufficiently strong constraints. This finding is in stark contrast to the case of the pressure in a thermal bath, which does not rely on the probe dynamics. In order to uniquely measure a constraint-independent pressure, the probe must be big enough so that the probe dynamics is much slower than the active particle. Our results greatly advance the understanding of active mechanical pressure on the probe, particularly for small probes in active bath, and have important implications for exploring the active pressure in complex viscoelastic environments.

Data availability statement

All data that support the findings of this study are included within the article (and any supplementary files).

Acknowledgments

We thank Ke Chen, Fangfu Ye and Rui Liu for helpful discussions. We acknowledge the supports of the National Natural Science Foundation of China (Nos. 12274448, 12047552), and the China Postdoctoral Science Foundation (No. 2022M723116).

ORCID iD

Peng Liu  <https://orcid.org/0000-0002-0898-584X>

References

- [1] Zhang H P, Be'er A, Florin E L and Swinney H L 2010 *Proc. Natl Acad. Sci. USA* **107** 13626
- [2] Wioland H, Woodhouse F G, Dunkel J, Kessler J O and Goldstein R E 2013 *Phys. Rev. Lett.* **110** 268102
- [3] Di Leonardo R, Angelani L, Dell'Arciprete D, Ruocco G, Iebba V, Schippa S, Conte M P, Mecarini F, De Angelis F and Di Fabrizio E 2010 *Proc. Natl Acad. Sci. USA* **107** 9541
- [4] Paxton W F, Kistler K C, Olmeda C C, Sen A, St. Angelo S K, Cao Y, Mallouk T E, Lammert P E and Crespi V H 2004 *J. Am. Chem. Soc.* **126** 13424
- [5] Sokolov A, Aranson I S, Kessler J O and Goldstein R E 2007 *Phys. Rev. Lett.* **98** 158102
- [6] Jiang H-R, Yoshinaga N and Sano M 2010 *Phys. Rev. Lett.* **105** 268302
- [7] Sokolov A and Aranson I S 2012 *Phys. Rev. Lett.* **109** 248109
- [8] Theurkauff I, Cottin-bizonne C, Palacci J, Ybert C and Bocquet L 2012 *Phys. Rev. Lett.* **108** 268303
- [9] Palacci J, Sacanna S, Steinberg A P, Pine D J and Chaikin P M 2013 *Science* **339** 936
- [10] Dey K K, Zhao X, Tansi B M, Méndez-Ortiz W J, Córdova-Figueroa U M, Golestanian R and Sen A 2015 *Nano Lett.* **15** 8311
- [11] Marchetti M C, Joanny J F, Ramaswamy S, Liverpool T B, Prost J, Rao M and Simha R A 2013 *Rev. Mod. Phys.* **85** 1143
- [12] Elgeti J, Winkler R G and Gompper G 2015 *Rep. Prog. Phys.* **78** 056601
- [13] Bechinger C, Leonardo R D, Löwen H, Reichhardt C, Volpe G and Volpe G 2016 *Rev. Mod. Phys.* **88** 045006
- [14] Gao W, Pei A, Feng X, Hennessy C and Wang J 2013 *J. Am. Chem. Soc.* **135** 998
- [15] Stenhammar J, Wittkowski R, Marenduzzo D and Cates M E 2015 *Phys. Rev. Lett.* **114** 018301
- [16] Takatori S C and Brady J F 2015 *Soft Matter* **11** 7920
- [17] Dolai P, Simha A and Mishra S 2018 *Soft Matter* **14** 6137
- [18] Angelani L 2019 *J. Phys.: Condens. Matter* **31** 075101
- [19] Wu X-L and Libchaber A 2000 *Phys. Rev. Lett.* **84** 3017
- [20] Peng Y, Lai L, Tai Y-S, Zhang K, Xu X and Cheng X 2016 *Phys. Rev. Lett.* **116** 068303
- [21] Loi D, Mossa S and Cugliandolo L F 2008 *Phys. Rev. E* **77** 051111
- [22] Palacci J, Cottin-Bizonne C, Ybert C and Bocquet L 2010 *Phys. Rev. Lett.* **105** 088304
- [23] Loi D, Mossa S and Cugliandolo L F 2011 *Soft Matter* **7** 3726
- [24] Szamel G 2014 *Phys. Rev. E* **90** 012111
- [25] Takatori S C, Yan W and Brady J F 2014 *Phys. Rev. Lett.* **113** 028103
- [26] Ginot F, Theurkauff I, Levis D, Ybert C, Bocquet L, Berthier L and Cottin-Bizonne C 2015 *Phys. Rev. X* **5** 011004
- [27] Speck T 2016 *Europhys. Lett.* **114** 30006
- [28] Fodor E, Nardini C, Cates M E, Tailleur J, Visco P and van Wijland F 2016 *Phys. Rev. Lett.* **117** 038103
- [29] Mandal D, Klymko K and DeWeese M R 2017 *Phys. Rev. Lett.* **119** 258001
- [30] Giannini J A and Puckett J G 2020 *Phys. Rev. E* **101** 062605
- [31] Bottinelli A and Silverberg J L 2017 *Front. Appl. Math. Stat.* **3** 26
- [32] Kulkarni A, Thampi S P and Panchagnula M V 2019 *Phys. Rev. Lett.* **122** 048002
- [33] Kaiser A, Peshkov A, Sokolov A, ten Hagen B, Löwen H and Aranson I S 2014 *Phys. Rev. Lett.* **112** 158101
- [34] Yan W and Brady J F 2015 *J. Fluid Mech.* **785** R1
- [35] Saintillan D 2018 *Annu. Rev. Fluid Mech.* **50** 563
- [36] Mallory S A, Valeriani C and Cacciuto A 2018 *Annu. Rev. Phys. Chem.* **69** 59
- [37] Yang Y and Bevan M A 2020 *Sci. Adv.* **6** eaay7679
- [38] Yang X, Bi D, Czajkowski M, Merkel M, Manning M L and Marchetti M C 2017 *Proc. Natl Acad. Sci. USA* **114** 12663
- [39] Takatori S and Brady J 2017 *Phys. Rev. Lett.* **118** 018003
- [40] Bialké J, Siebert J T, Löwen H and Speck T 2015 *Phys. Rev. Lett.* **115** 098301
- [41] Zakine R, Zhao Y, Knežević M, Daerr A, Kafri Y, Tailleur J and van Wijland F 2020 *Phys. Rev. Lett.* **124** 248003
- [42] Omar A K, Wang Z-G and Brady J F 2020 *Phys. Rev. E* **101** 012604
- [43] Solon A P, Stenhammar J, Wittkowski R, Kardar M, Kafri Y, Cates M E and Tailleur J 2015 *Phys. Rev. Lett.* **114** 198301
- [44] Winkler R G, Wysocki A and Gompper G 2015 *Soft Matter* **11** 6680
- [45] Grosberg A and Joanny J-F 2015 *Phys. Rev. E* **92** 032118
- [46] Speck T, Menzel A M, Bialké J and Löwen H 2015 *J. Chem. Phys.* **142** 224109
- [47] Blaschke J, Maurer M, Menon K, Zöttl A and Stark H 2016 *Soft Matter* **12** 9821
- [48] Takatori S C and Brady J F 2016 *Curr. Opin. Colloid Interface Sci.* **21** 24
- [49] Prymidis V, Paliwal S, Dijkstra M and Fillion L 2016 *J. Chem. Phys.* **145** 124904
- [50] Rein M and Speck T 2016 *Eur. Phys. J. E* **39** 84
- [51] Levis D, Codina J and Pagonabarraga I 2017 *Soft Matter* **13** 8113
- [52] Lee C F 2017 *Soft Matter* **13** 376
- [53] Patch A, Yllanes D and Marchetti M C 2017 *Phys. Rev. E* **95** 012601
- [54] Bazant M Z 2017 *Faraday Discuss.* **199** 423
- [55] Omar A K, Wu Y, Wang Z-G and Brady J F 2018 *ACS Nano* **13** 560
- [56] Digregorio P, Levis D, Suma A, Cugliandolo L F, Gonnella G and Pagonabarraga I 2018 *Phys. Rev. Lett.* **121** 098003
- [57] Solon A P, Stenhammar J, Cates M E, Kafri Y and Tailleur J 2018 *Phys. Rev. E* **97** 020602
- [58] Solon A P, Stenhammar J, Cates M E, Kafri Y and Tailleur J 2018 *New J. Phys.* **20** 075001
- [59] Paliwal S, Rodenburg J, van Roij R and Dijkstra M 2018 *New J. Phys.* **20** 015003
- [60] Yan W, Zhang H and Shelley M J 2019 *J. Chem. Phys.* **150** 064109
- [61] van der Meer B, Prymidis V, Dijkstra M and Fillion L 2020 *J. Chem. Phys.* **152** 144901
- [62] Speck T 2020 *Soft Matter* **16** 2652
- [63] Baglietto G, Seif A, Grigera T and Paul W 2020 *Phys. Rev. E* **101** 062606
- [64] Solon A P, Fily Y, Baskaran A, Cates M E, Kafri Y, Kardar M and Tailleur J 2015 *Nat. Phys.* **11** 673

- [65] Wysocki A, Elgeti J and Gompper G 2015 *Phys. Rev. E* **91** 050302
- [66] Speck T and Jack R L 2016 *Phys. Rev. E* **93** 062605
- [67] Zöttl A and Stark H 2016 *J. Phys.: Condens. Matter* **28** 253001
- [68] Marchetti M C, Fily Y, Henkes S, Patch A and Yllanes D 2016 *Curr. Opin. Colloid Interface Sci.* **21** 34
- [69] Paoluzzi M, Di Leonardo R, Marchetti M C and Angelani L 2016 *Sci. Rep.* **6** 34146
- [70] Joyeux M and Bertin E 2016 *Phys. Rev. E* **93** 032605
- [71] Takatori S C, De Dier R, Vermant J and Brady J F 2016 *Nat. Commun.* **7** 10694
- [72] Junot G, Briand G, Ledesma-Alonso R and Dauchot O 2017 *Phys. Rev. Lett.* **119** 028002
- [73] Fily Y, Kafri Y, Solon A P, Tailleur J and Turner A 2018 *J. Phys. A: Math. Theor.* **51** 044003
- [74] Quillen A, Smucker J and Peshkov A 2020 *Phys. Rev. E* **101** 052618
- [75] Yan W and Brady J F 2015 *Soft Matter* **11** 6235
- [76] Marconi U M B, Maggi C and Melchionna S 2016 *Soft Matter* **12** 5727
- [77] Smallenburg F and Löwen H 2015 *Phys. Rev. E* **92** 032304
- [78] Nikola N, Solon A P, Kafri Y, Kardar M, Tailleur J and Voituriez R 2016 *Phys. Rev. Lett.* **117** 098001
- [79] Jamali T and Naji A 2018 *Soft Matter* **14** 4820
- [80] Liu P, Ye S, Ye F, Chen K and Yang M 2020 *Phys. Rev. Lett.* **124** 158001
- [81] Ye S, Liu P, Ye F, Chen K and Yang M 2020 *Soft Matter* **16** 4655
- [82] Ye S, Liu P, Wei Z, Ye F, Yang M and Chen K 2020 *Chin. Phys. B* **29** 058201
- [83] Li L, Liu P, Chen K, Zheng N and Yang M 2022 *Soft Matter* **18** 4265
- [84] Paul S, Jayaram A, Narinder N, Speck T and Bechinger C 2022 *Phys. Rev. Lett.* **129** 058001
- [85] Cates M E and Tailleur J 2015 *Annu. Rev. Condens. Matter Phys.* **6** 219
- [86] Yang M and Ripoll M 2013 *Phys. Rev. E* **87** 062110
- [87] Saintillan D and Shelley M J 2015 *Complex Fluids in Biological Systems* (Springer) pp 319–55